A study of the radiological baseline conditions around the planned Sinop (Turkey) nuclear power plant using the mapping method

Hasan Baltas · Cafer Mert Yesilkanat · Erkan Kiris · Murat Sirin

Abstract This study makes a first attempt at a detailed estimation of the background radioactivity level and its distribution at the Sinop nuclear power plant site. The activity concentration levels of ^{226}Ra, ^{232}Th, ^{40}K and ^{137}Cs radionuclides in soil samples collected from 88 locations around Sinop Province, Turkey, in November 2016, were measured using gamma spectrometry. The distributions of radionuclide levels obtained from the results were evaluated using a geostatistical method, and the estimated radiation levels were determined using the ordinary kriging (OK) method, which is the best linear unbiased estimator (BLUE) for unmeasured points. Estimates of distribution results were evaluated using cross-validation diagrams, and it was shown that the OK method could predict radiological distributions for appropriate criteria. Finally, using the kriging parameters, distributions of radiation levels for the entire work area were mapped at a spatial resolution of 100×100 m^2. These maps show that the natural radionuclides (^{226}Ra, ^{232}Th and ^{40}K) are distributed at higher levels to the southeast of Sinop than in the other regions, and the activity of an artificial radionuclide (^{137}Cs) is high in the interior and northern sections.

Introduction

In the increasingly developing world, power plays a fundamental role in the process of economic growth and development. All countries in the world aim to achieve a cost-effective, reliable and safe electricity source to sustain modern ways of living (Brahmanandhan et al. 2007). In developing countries such as Turkey, the demand for electricity is constantly increasing, and to sustain the economy, long-term planning is needed. The Turkish Atomic Energy Commission (TAEC) is planning to install a nuclear power plant (NPP) (four ATMEA1 reactors, each of 1120 MWe) within the Sinop Province (İnceburun) in northern Turkey (Fig. 1).

The human being is intertwined with radiation in its environment and is exposed to natural radioactivity continuously. It is present in our environment due to the cosmogenic and primordial radionuclides present in the Earth's crust. External exposure of living organisms to natural and artificial radioactivity due to the region where they live differs according to the geological and geographic conditions of the investigated region and occurs at different levels in the soil of different regions around the world (UNSCEAR 2000).

The main reason for the presence of artificial radionuclides in the environment is due to nuclear anthropogenic activities including weapons, industry, medical and energy. Soil is the main terrestrial ecosystem that

H. Baltas (✉) · E. Kiris · M. Sirin
Department of Physics, Faculty of Arts and Science, Recep Tayyip Erdoğan University, 53100 Rize, Turkey
e-mail: hasan.baltas@erdogan.edu.tr

C. M. Yesilkanat
Science Teaching Department, Faculty of Education, Artvin Çoruh University, 08000 Artvin, Turkey
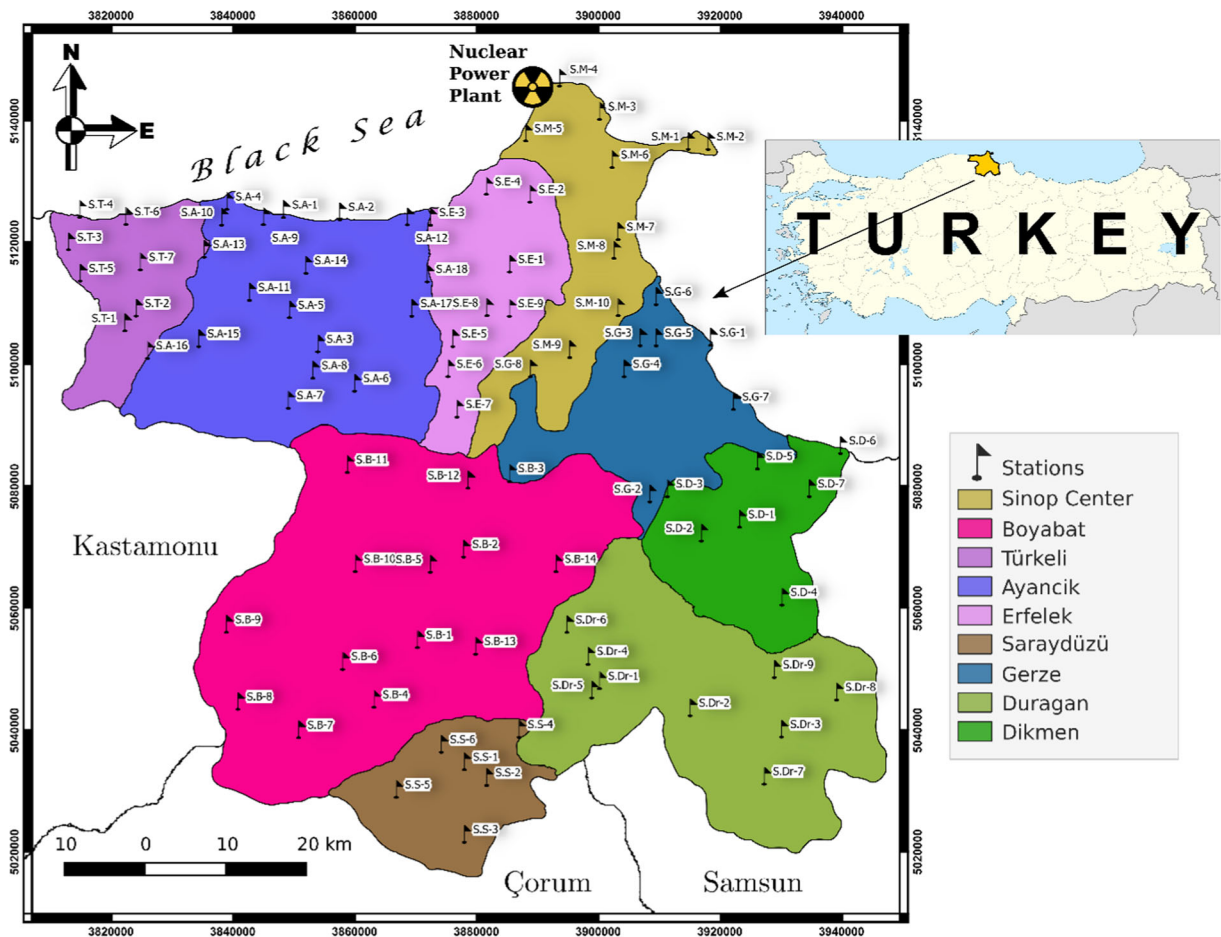
Fig. 1 The study area and sampling stations

detains and holds natural and anthropogenic (artificial) pollutants in its structure (Lukšienė et al. 2012). Radioactive substances occurring after a nuclear accident may spread across the continents and across the world, causing great damage to the environment and long-term permanent effects (Leelőssy et al. 2011). At the same time, with the increasing use of NPPs around the world due to increased energy demand, there is often the possibility of exposure to radioactive contamination in neighbouring countries (Mičieta and Murín 2007).

Determining the distribution of naturally or artificially radioactive nuclides that are present in the environment is necessary for assessing the effects of radiation exposure for public health (Kam et al. 2010). Monitoring of radioactivity in soil is very important to determine any changes in activity with time as a result of radioactive release (Kurnaz et al. 2011). Transfer of radionuclides present in the soil into the air and the food chain causes intake of systemic doses in the living organisms and human population

(Kayakökü and Doğru 2017). Soil is one of the major sources of radiation exposure to a population via the transfer of radionuclides into the environment (Durusoy and Yildirim 2017). In this way, soil contributes significantly to the internal and external exposures to environmental radioactivity by gamma rays that increase the risk to human health (Elsaman et al. 2018). For this reason, measurements of natural and artificial radioactivity in soil samples are continuously carried out by many researchers in Turkey and many other countries (Kam et al. 2010; Kurnaz et al. 2011; Lukšienė et al. 2012; El Samad et al. 2013; Karadeniz et al. 2015; Yeşilkanat et al. 2015; Durusoy and Yildirim 2017; Kayakökü and Doğru 2017).

Before and after the construction of a NPP, it is critical to monitor the environmental radiation in the soil samples around the NPP and to assess the dose rates to which people receive. Such monitoring is very useful in assessing the possible radiological risks to public health in the area where the power plant is installed before a

power plant is installed, and for the guarantee of normality during commercial operation (Tsai et al. 2008).

The present work aims to estimate the activity concentration of the radionuclides ^{226}Ra, ^{232}Th and ^{40}K and the man-made radionuclide ^{137}Cs in soil samples collected from the terrestrial area of the Sinop Province for which the NPP is planned, and to evaluate the radiological indices and their effects on the population within this environment. Consequently, the results of the radioactivity concentration obtained in this study will provide background information for the current radioecological condition in Sinop before any new NPP is established and started to operate.

Materials and methods

Study area and sampling

Sinop is a peninsula located in the Boztepe Peninsula, which extends towards the north of the Black Sea coastline. It is located in the central Black Sea region (41° 36′ 33″ N, 34° 54′ 07″ E). The surface area is 5862 km^2, equivalent to 0.8% of Turkey's surface area. The total length of its borders is 475 km, 300 km of these borders are land borders and 175 km coastal borders. It is surrounded by Kastamonu in the west, Çorum in the south, Samsun in the southeast and Karadeniz in the north.

In November 2016, a total of 88 surface soil samples from nine major sites were collected at a depth of 0–10 cm randomly from the city centre and from around the proposed NPP site (Fig. 1). The nine sites were Sinop city centre (10 samples), Ayancık (18 samples), Boyabat (14 samples), Dikmen (seven samples), Durgan (nine samples), Erfelek (nine samples), Gerze (eight samples), Saraydüzü (six samples) and Türkeli (seven samples). All of the samples were collected following standard procedures as per IAEA guidelines (Holm and Ballestra 1989).

Radioactivity measurements

The soil samples were dried in a temperature-controlled oven at 85 ° C for 24 h to remove the moisture and water contained therein. The dried samples were crushed in porcelain mortar and mixed well. Then, all samples were passed through a 63-μm (400 mesh) sieve to homogenize the particle size of the samples. About 120 g of each sample was sealed in a gas-tight, radon-impermeable, cylindrical polyethylene plastic container (5.5 cm diameter, 5 cm height) for gamma activity

analysis. Before measurements were taken, the containers were kept sealed for 4 weeks, in order to reach an equilibrium between ^{226}Ra and its short-lived progeny (Baltas et al. 2014).

The activity concentrations of ^{226}Ra, ^{232}Th, ^{40}K and ^{137}Cs in all samples were measured using a coaxial HPGe detector of 55% relative efficiency and a resolution of 1.9 keV at the 1332 keV gamma of ^{60}Co (Ortec, GEM55P4-95 model). A detailed description of the detector characteristics, system operation, calibration and the gamma lines used to determine the activity concentration of ^{226}Ra, ^{232}Th, ^{40}K and ^{137}Cs has been presented elsewhere (Baltas et al. 2014; Baltas et al. 2017; Baltas et al. 2018).

The activity concentration values for the radionuclides in the measured samples were computed using the following equation:

$$C = \frac{N}{\varepsilon \times P_\gamma \times m} \quad (\text{Bq kg}^{-1}) \tag{1}$$

where N is the net count per second for the gamma emission; ε is the photopeak efficiency of the used detector; P_γ is the abundance of the gamma line in a radionuclide, the absolute transition for gamma decay; and m is the weight of the dried sample in kilogrammes (Baltas et al. 2018).

The minimum detectable activity (MDA) of this measurement system was calculated as follows (Currie 1968):

$$\text{MDA} = \frac{\sigma\sqrt{B}}{\varepsilon \times P_\gamma \times T \times m} \tag{2}$$

where MDA is expressed in becquerels per kilogramme; σ is the statistical coverage factor, which is equal to 1.645 (confidence level 95%); B is the background for the region of interest of a certain radionuclide; and T is the counting time in seconds (Baltas et al. 2018). The MDA for the radionuclides of interest was calculated as 0.16, 0.24, 1.69 and 0.02 Bq kg^{-1} for ^{226}Ra, ^{232}Th, ^{40}K and ^{137}Cs, respectively. In IAEA-447-coded certified reference material sample, ^{226}Ra, ^{232}Th, ^{137}Cs and ^{40}K activity concentrations are given as 25.04, 37.3, 371.11 and 550 Bq kg^{-1}, respectively. The activity concentrations of ^{226}Ra, ^{232}Th, ^{137}Cs and ^{40}K for the counting system were calculated as 23.96, 35.7, 362.55 and 521 Bq kg^{-1}, respectively. Accuracy, expressed as recovery of reference material, was 95–98% for all

Table 1 Statistical summary of activity levels of radionuclides for each district

	Statistic Summary	Center (N=10)	Ayancık (N=18)	Boyabat (N=14)	Dikmen (N=7)	Duragan (N=9)	Erfelek (N=9)	Gerze (N=8)	Saraydüzü (N=6)	Türkeli (N=7)	All Study Area (N=88)
^{226}Ra (Bq kg^{-1})	Min.	3.61	8.62	6.47	12.83	13.58	7.43	10.21	7.12	9.09	3.61
	Max.	41.07	17.94	25.21	25.37	27.63	20.77	19.02	12.62	18.46	41.07
	Mean	15.05	12.72	13.97	16.64	20.04	12.23	13.91	11.01	13.17	14.22
	Stand. dev	10.48	2.43	5.99	4.85	5.58	4.75	2.47	1.96	4.09	5.66
	Median	12.21	12.60	14.19	17.01	17.86	9.89	13.58	11.62	11.52	13.00
	Skewness	1.86	0.26	0.58	0.72	0.19	1.05	0.10	-2.17	0.32	1.63
	Kurtosis	4.39	-0.27	-0.13	1.13	-2.06	-0.17	-2.00	5.09	-2.32	2.06
^{232}Th (Bq kg^{-1})	Min.	4.55	9.30	5.29	17.56	20.39	9.24	13.30	2.45	11.94	2.45
	Max.	26.66	26.25	38.51	49.26	40.72	36.80	30.93	16.82	23.15	49.26
	Mean	17.10	17.24	19.37	24.27	27.80	17.18	18.15	12.51	16.89	18.93
	Stand. dev	6.09	3.69	9.43	12.25	7.42	8.25	4.00	5.63	3.86	7.78
	Median	16.87	17.65	19.00	18.19	25.52	14.81	17.56	14.96	15.27	17.55
	Skewness	-0.58	0.08	0.59	1.78	0.69	1.94	0.55	-1.46	0.64	1.25
	Kurtosis	1.28	1.83	0.14	3.05	-0.83	4.39	-0.62	1.42	-0.37	2.85
^{40}K (Bq kg^{-1})	Min.	65.40	118.50	127.00	260.70	292.30	153.10	192.20	50.60	197.50	50.60
	Max.	673.20	371.10	485.70	467.10	519.80	373.50	362.70	258.30	368.90	673.20
	Mean	240.03	267.23	285.31	334.14	394.63	255.87	275.35	181.53	261.21	278.62
	Stand. dev	51.92	16.43	26.24	26.70	32.84	28.15	23.22	30.29	21.69	10.94
	Median	216.20	283.95	288.45	320.30	342.30	241.90	288.70	198.60	257.00	269.90
	Skewness	2.32	-0.65	0.29	1.05	0.32	0.12	-0.22	-1.21	0.97	0.82
	Kurtosis	6.57	-0.46	-0.25	1.56	-2.23	-1.51	-1.99	1.52	1.65	2.01
^{137}Cs (Bq kg^{-1})	Min.	2.31	1.16	1.16	4.01	1.46	1.06	0.51	0.96	0.48	0.48
	Max.	15.60	26.00	12.83	11.19	6.95	27.92	9.83	5.19	8.68	27.92
	Mean	7.26	4.61	4.18	3.33	2.28	5.52	4.61	2.81	3.35	4.37
	Stand. dev	4.79	6.21	4.05	3.59	1.90	8.72	2.85	1.27	2.94	4.88
	Median	7.08	2.07	1.85	1.80	1.50	1.70	3.97	2.35	1.92	2.11
	Skewness	0.34	2.78	1.42	2.31	2.31	2.63	0.92	1.73	1.42	2.72
	Kurtosis	-0.81	8.49	0.91	5.45	5.39	7.18	0.06	2.97	0.44	9.26

of the radionuclides. The specific activities of soil samples were in accordance with their certified values, within errors of the order of 3–7%.

Geostatistic analysis and interpolated mapping

Geostatistics is a statistical analysis technique that determines the relationship between spatial samples, not only by using the statistical properties of samples but also by taking into account the coordinates of samples taken at the same time. The most important advantage of this calculation method is that the size of the error in the calculation can be determined within certain confidence intervals (Clark 1979). Thus, measurement results from a specific area are only specific to the sampled stations. It is generally necessary to interpolate unknown values for unsampled intermediate stations, in order to determine the distribution of the results. The similarity between the results of measurements using geostatistical methods is defined as a function of the distances between the stations, and unbiased and minimum variance estimations can be made by considering this function (Matheron 1970; Olea 1982). In geostatistics, the distance-dependent variations of regional variables are determined by the variogram function, and this function is expressed as the variance of the difference between two variables spaced apart by h (Webster and Oliver 2001). As the distance between the variables increases, the differences between the values of the variables increase, and
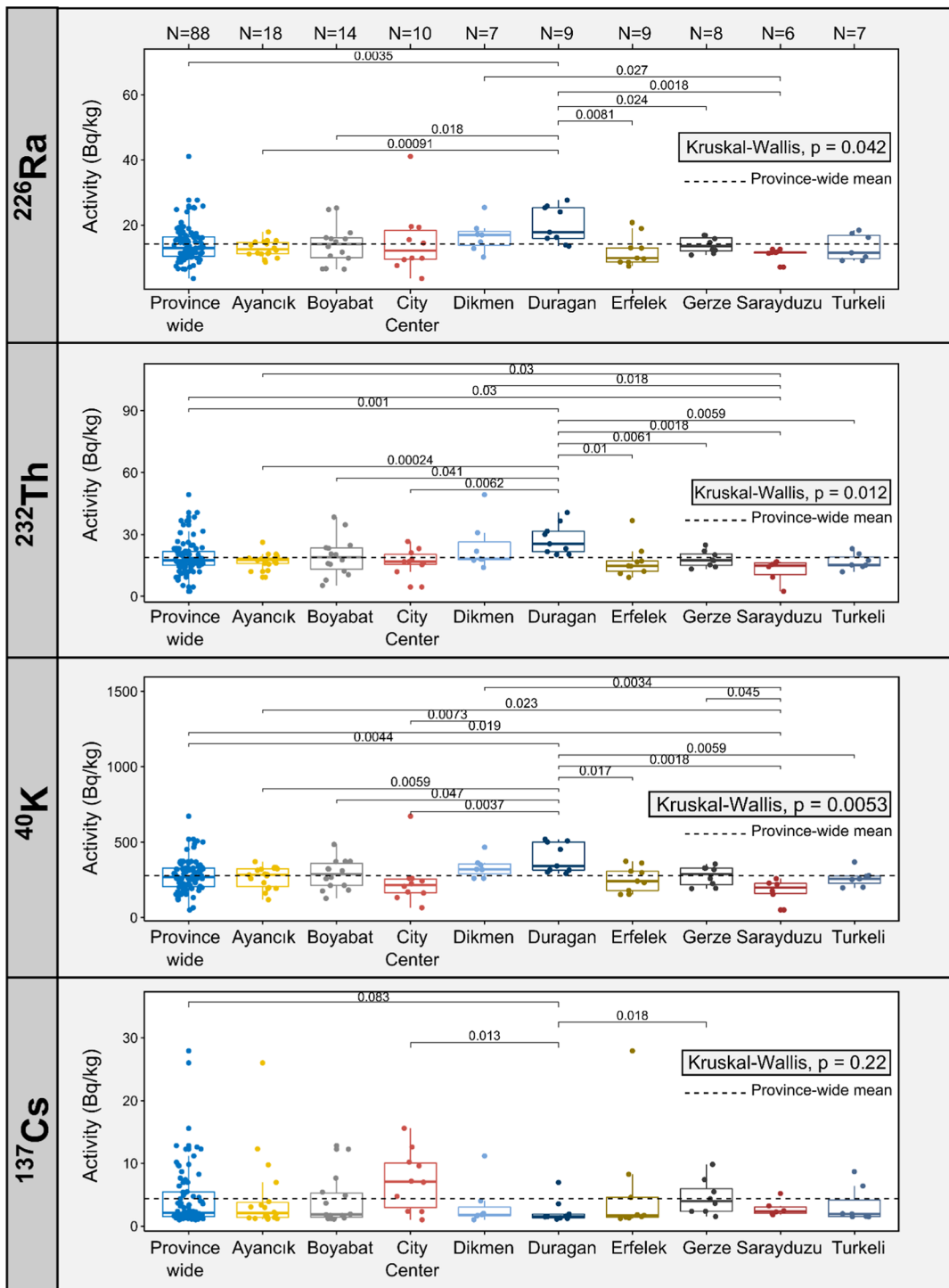
Fig. 2 Activity levels of radionuclides, using a box whisker plot for each district

thus, the variance (semivariance) increases. This increase in variance can be interpreted as a decrease in the relationship between the variables (Diggle and Ribeiro Jr 2007). Semivariance is a measure of the degree of spatial dependence between samples. The semivariance for the entire

space is determined by Eq. (3) (İnal and Yiğit 2003):

$$\gamma(h) = \frac{1}{2N(h)} \sum_{i=1}^{N(h)} \left(Z(x_i) - Z(x_i + h) \right)^2 \qquad (3)$$

where $\gamma(h)$ is semivariance value, h is distance between two measuring points, $N(h)$ is number of point pairs in the length h, $Z(x_i)$ is value of the variable at point i and $Z(x_i + h)$ is value of the variable measured at point $x_i + h$.

Despite the existence of many different methods (Oliver and Webster 2014) that can be used for various purposes in geostatistical analysis, this metric is generally referred to as the weighted average calculation and is the best linear unbiased estimator (BLUE)

in the literature (Matheron 1970; Krige 1966), where the ordinary kriging (OK) method is used. In geostatistical analysis, any non-uniformity in the distribution leads to miscalculation of the kriging weights by distorting the structure of the variogram. Thus, experimental data that are often log-normal are applied to data transformations to ensure a normal distribution fit (Krige 1966; Li et al. 2009; Yeşilkanat et al. 2015). In recent years, this method has often been used to determine the radiological distribution (Yeşilkanat et al. 2015; Cafaro et al. 2014; Hiemstra et al. 2009; Kobya et al. 2015; Kucukomeroglu et al. 2016; Sanusi et al. 2014; Savelieva 2005; Warnery et al. 2015).

All statistical analyses and interpolation estimations used in this study were carried out in the R
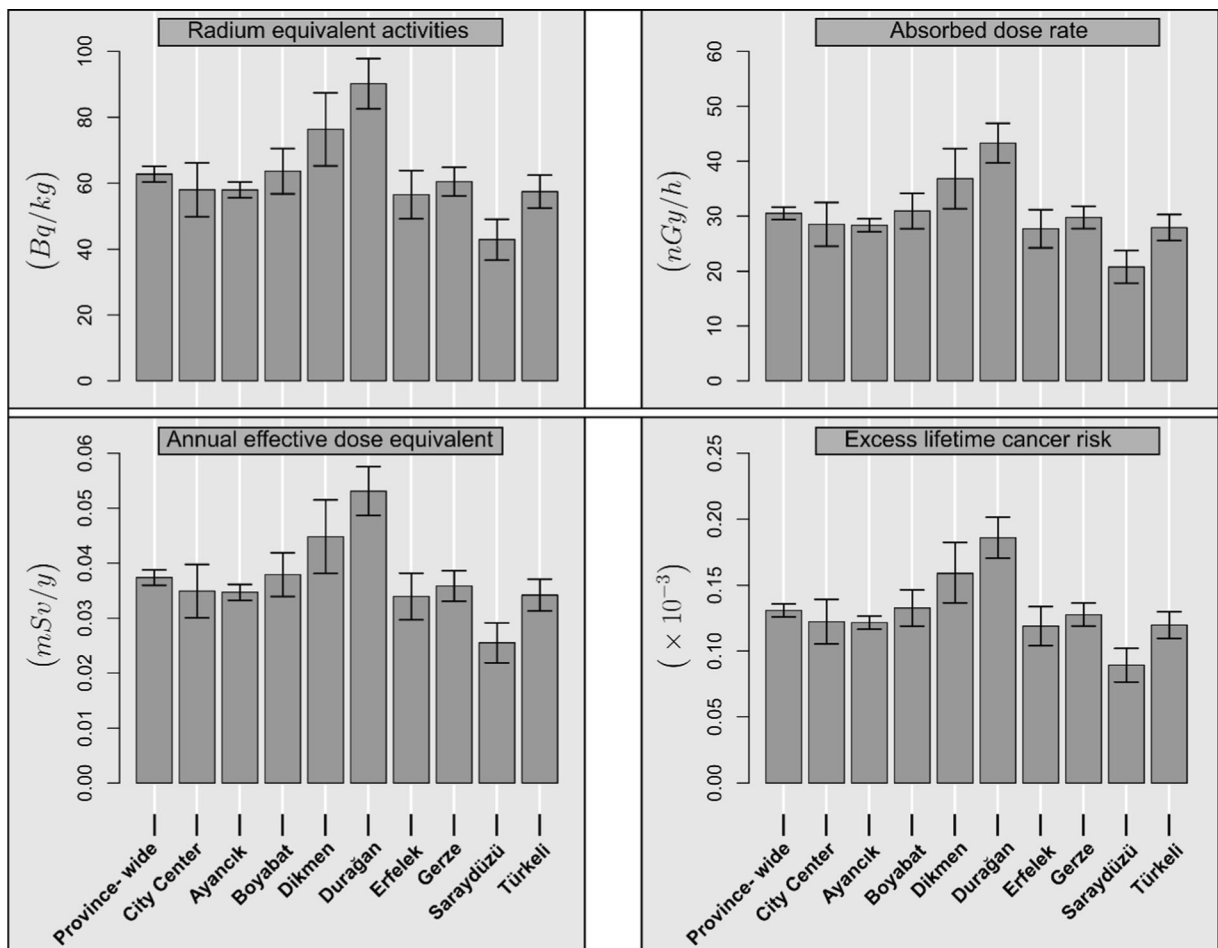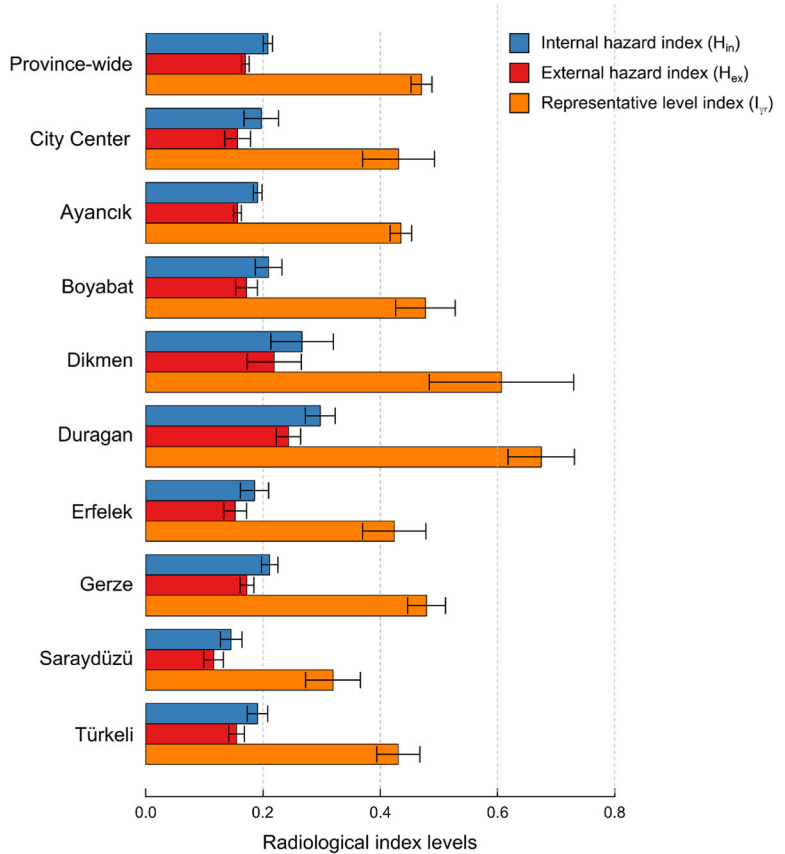

Fig. 3 Mean values (± SD) of Ra$_{eq}$, D_R, AEDE and ELCR radiological risk levels for each district in the study area

Fig. 4 Mean values (± SD) of the H_{in}, H_{ex} and $I_{\gamma r}$ radiological risk indices for each district in the study area

Results and discussion

^{226}Ra, ^{232}Th, ^{40}K and ^{137}Cs activity concentrations

Table 1 shows a statistical summary of the ^{226}Ra, ^{232}Th, ^{40}K and ^{137}Cs activity levels for each district, based on the soil samples taken from the stations shown in Fig. 1. According to the findings from the measurements, the average activity concentrations in Sinop Province were determined as 14.22 Bq kg^{-1} for ^{226}Ra, 18.93 Bq kg^{-1} for ^{232}Th, 278.62 Bq kg^{-1} for ^{40}K and 4.37 Bq kg^{-1} for

programming language (Ihaka and Gentleman 1996; Team 2005). R is an open source language, and a free version of the S programming language is available under the general public license (GPL). The *GSTAT* (Pebesma and Wesseling 1998) and *sp* (Pebesma and Bivand 2005) packages in R were used for geostatistical calculations.

^{137}Cs. The concentrations ranged from 3.61 to 41.07 Bq kg^{-1} for ^{226}Ra, 2.45 to 49.26 Bq kg^{-1} for ^{232}Th, 50.60 to 673.20 Bq kg^{-1} for ^{40}K and N.D. to 27.92 Bq kg^{-1} for ^{137}Cs. Figure 2 shows the variation in radionuclide levels using a box whisker plot for each district in the study area. A Kruskal-Wallis test was used to determine whether there was a significant difference between the radionuclide distributions and the sampling stations. A one-way analysis of variance could not be used in this study, since there were insufficient samples for each district. Significant differences ($p < 0.05$) were determined between districts, according to the results of the Kruskal-Wallis test for natural radionuclides. A Mann-Whitney pairwise comparison test was used to determine which of these differences were significant.

From the ^{226}Ra activity in Fig. 2, it was determined that the Saraydüzü district had a significantly different ($p < 0.05$) distribution from Dikmen, while the Durağan district showed a significantly different

Table 2 Statistical summary of parameters for radiological risk levels

	Statistic summary	Centre ($N=10$)	Ayancık ($N=18$)	Boyabat ($N=14$)	Dikmen ($N=7$)	Duragan ($N=9$)	Erfelek ($N=9$)	Gerze ($N=8$)	Saraydüzü ($N=6$)	Türkeli ($N=7$)	All study area ($N=88$)
Ra_{eq} (Bq kg^{-1})	Min.	15.15	34.36	27.68	50.33	67.01	32.52	44.67	14.52	41.41	14.52
	Max.	104.38	80.96	117.68	131.78	125.02	102.15	77.86	55.10	78.98	131.78
	Mean	57.98	57.94	63.64	77.07	90.18	56.49	61.07	42.87	57.43	62.74
	Stan. dev	25.77	10.23	25.76	27.11	22.93	21.98	12.32	15.12	13.18	22.47
	Median	53.22	59.01	63.50	67.74	78.77	52.47	58.63	48.50	53.01	60.11
H_{in}	Min.	0.05	0.12	0.09	0.16	0.22	0.11	0.15	0.06	0.14	0.05
	Max.	0.36	0.26	0.39	0.42	0.41	0.33	0.26	0.18	0.26	0.42
	Mean	0.20	0.19	0.22	0.25	0.30	0.19	0.20	0.15	0.19	0.21
	Stan. dev	0.09	0.03	0.08	0.09	0.08	0.07	0.04	0.05	0.05	0.07
	Median	0.18	0.20	0.21	0.23	0.26	0.17	0.19	0.16	0.17	0.20
H_{ex}	Min.	0.04	0.09	0.07	0.14	0.18	0.09	0.12	0.04	0.11	0.04
	Max.	0.28	0.22	0.32	0.36	0.34	0.28	0.21	0.15	0.21	0.36
	Mean	0.16	0.16	0.18	0.21	0.24	0.15	0.16	0.12	0.16	0.17
	Stan. dev	0.07	0.03	0.07	0.07	0.06	0.06	0.03	0.04	0.04	0.06
	Median	0.14	0.16	0.17	0.18	0.21	0.14	0.16	0.13	0.14	0.16
$I_{\gamma r}$	Min.	0.11	0.26	0.21	0.38	0.50	0.24	0.33	0.11	0.31	0.11
	Max.	0.81	0.61	0.88	0.97	0.93	0.76	0.58	0.41	0.59	0.97
	Mean	0.43	0.44	0.48	0.58	0.67	0.42	0.46	0.32	0.43	0.47
	Stan. dev	0.19	0.08	0.19	0.20	0.17	0.16	0.09	0.11	0.10	0.17
	Median	0.40	0.44	0.48	0.51	0.59	0.39	0.44	0.36	0.40	0.45
D_R (nGy h^{-1})	Min.	7.51	16.71	13.72	24.56	32.34	15.78	21.59	7.22	20.13	7.22
	Max.	52.65	38.82	56.00	63.25	59.46	48.25	37.32	26.69	38.04	63.25
	Mean	28.50	28.32	30.93	37.14	43.30	27.69	29.78	20.79	27.90	30.51
	Stan. dev	12.57	5.02	12.09	12.87	10.87	10.42	5.98	7.27	6.27	10.67
	Median	26.86	29.44	30.59	33.23	38.22	25.31	28.84	23.40	25.77	29.80
AEDE (mSv year^{-1})	Min.	0.01	0.02	0.02	0.03	0.04	0.02	0.03	0.01	0.02	0.01
	Max.	0.06	0.05	0.07	0.08	0.07	0.06	0.05	0.03	0.05	0.08
	Mean	0.03	0.03	0.04	0.05	0.05	0.03	0.04	0.03	0.03	0.04
	Stan. dev	0.02	0.01	0.01	0.02	0.01	0.01	0.01	0.01	0.01	0.01
	Median	0.03	0.04	0.04	0.04	0.05	0.03	0.04	0.03	0.03	0.04
ELRC ($\times 10^{-3}$)	Min.	0.03	0.07	0.06	0.11	0.14	0.07	0.09	0.03	0.09	0.03
	Max.	0.23	0.17	0.24	0.27	0.26	0.21	0.16	0.11	0.16	0.27
	Mean	0.12	0.12	0.13	0.16	0.19	0.12	0.13	0.09	0.12	0.13
	Stan. dev	0.05	0.02	0.05	0.06	0.05	0.04	0.03	0.03	0.03	0.05
	Median	0.12	0.13	0.13	0.14	0.16	0.11	0.12	0.10	0.11	0.13

($p < 0.05$) distribution from Ayancık, Boyabat, Erfelek, Gerze, Saraydüzü and province as a whole. For [232]Th activity, it was determined that the Saraydüzü district had a significantly different ($p < 0.05$) distribution from Dikmen, Ayancık and the province as a whole, while the Durağan district

showed a significant difference ($p < 0.05$) from all districts except Dikmen and the province overall. Likewise, for [40]K activity, it was found that the Saraydüzü district had a significantly different ($p < 0.05$) distribution from Dikmen, Gerze, Ayancık and the province as a whole, while Durağan showed a
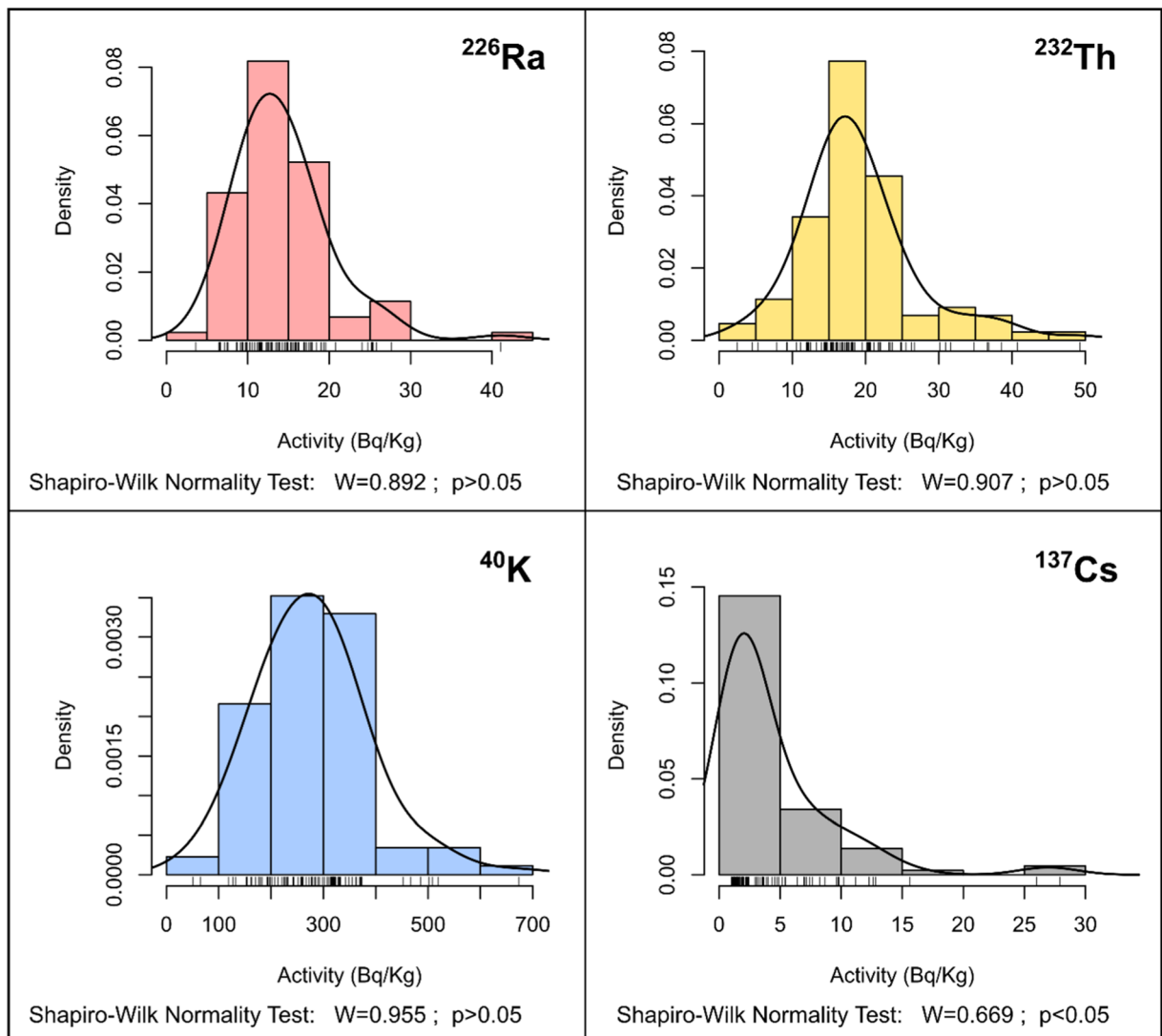
Fig. 5 Histograms for each radionuclide

significant difference ($p < 0.05$) from all districts except Dikmen and the province overall. These differences in natural radionuclides are thought to be due to geological rock formations and the variability in soil structure (Abba et al. 2017; Hung et al. 2016). Although the ^{137}Cs radionuclide distribution was not significantly different from the Kruskal-Wallis test ($p > 0.05$), the Mann-Whitney pairwise comparison showed a statistically significant difference ($p < 0.05$) between the city centre of the Durağan district, Gerze and the province as a whole. The high activity value of the coastal areas compared with that of the inner regions, due to the

Chernobyl NPP accident, was considered to be the source of this regional difference in the distribution of the artificial radionuclide.

Radiological risk levels

There are many parameters that arise from radionuclides and which indicate hazard criteria for radioactivity. The parameters most used in the literature are the radium equivalent (Ra_{eq}), absorbed dose rate (D_R), annual effective dose equivalent (AEDE), excess lifetime cancer risk (ELCR), internal hazard index (H_{in}), external hazard index (H_{ex}) and gamma representative level index

($I_{\gamma r}$). These radiological risk levels can be calculated using the following equations (UNSCEAR 2000; Beretka and Mathew 1985; ICRP 1991; Krieger 1981):

$$D_R\left(nGy\ h^{-1}\right) = 0.461A_{Ra} + 0.623A_{Th}$$
$$+ 0.0417A_K + 0.1243A_{Cs} \tag{5}$$

$$Ra_{eq}\left(Bq\ kg^{-1}\right) = A_{Ra} + 1.43A_{Th} + 0.077A_K \tag{4}$$

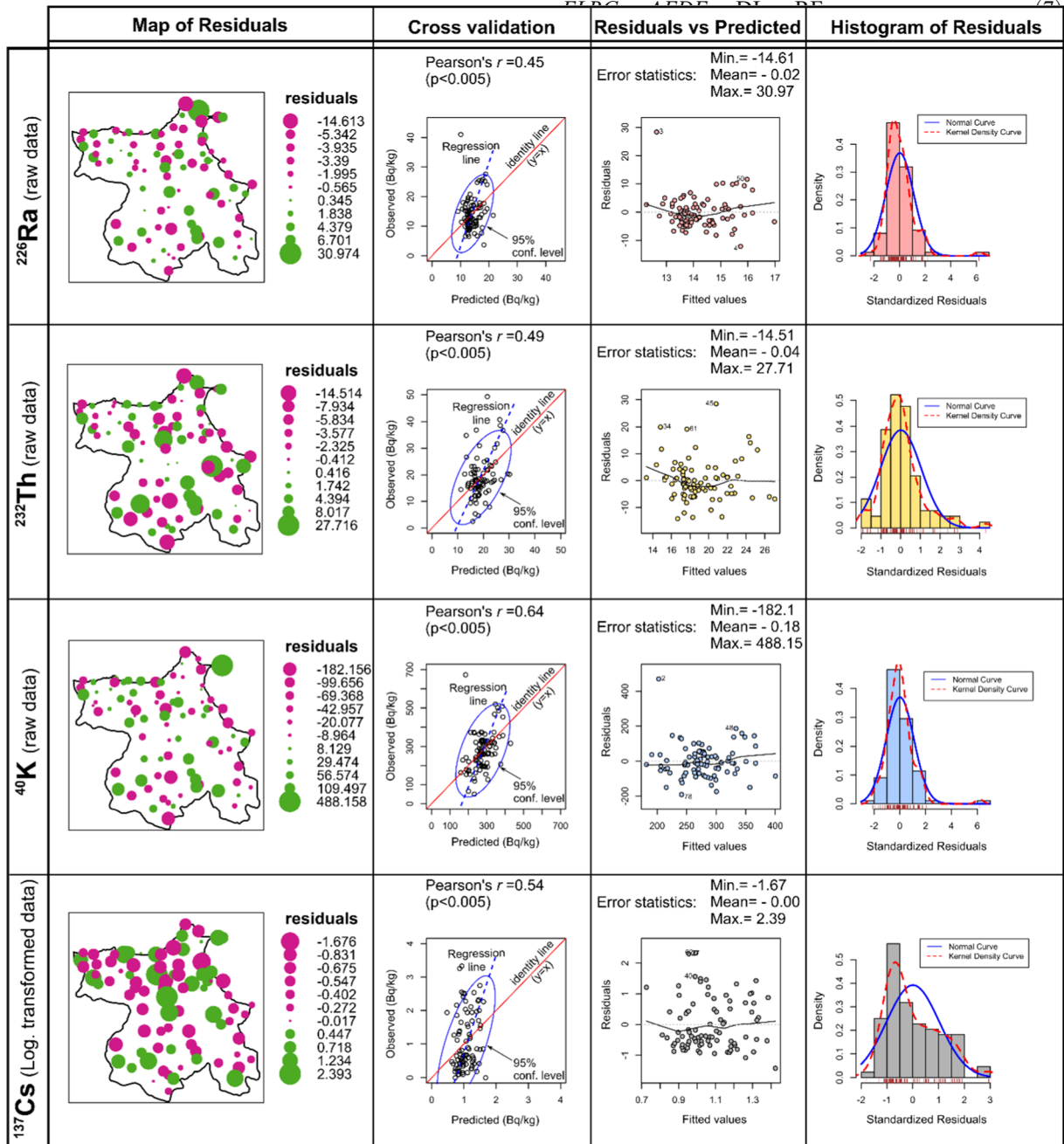$$AEDE\left(mSv\ year^{-1}\right) = D_R \times DCF \times OF \times T \tag{6}$$

Fig. 6 Cross-validation diagrams for radionuclides

$$H_{in} = \frac{A_{Ra}}{185 \text{ Bq kg}^{-1}} + \frac{A_{Th}}{259 \text{ Bq kg}^{-1}}$$
$$+ \frac{A_K}{4810 \text{ Bq kg}^{-1}} \quad\quad (8)$$

$$H_{ex} = \frac{A_{Ra}}{370 \text{ Bq kg}^{-1}} + \frac{A_{Th}}{259 \text{ Bq kg}^{-1}}$$
$$+ \frac{A_K}{4810 \text{ Bq kg}^{-1}} \quad\quad (9)$$

$$I_{\gamma r} = \frac{A_{Ra}}{150 \text{ Bq kg}^{-1}} + \frac{A_{Th}}{100 \text{ Bq kg}^{-1}}$$
$$+ \frac{A_K}{1500 \text{ Bq kg}^{-1}} \quad\quad (10)$$

where A_{Ra}, A_{Th} and A_K are the activity concentrations (Bq kg^{-1}) of ^{226}Ra, ^{232}Th and ^{40}K, respectively, in the soil sample, D_R is the absorbed dose rate in air, DCF is the dose conversion factor (0.7 Sv Gy^{-1}), OF is the outdoor occupancy factor (0.2), T is the time (8760 h year^{-1}), DL is the average duration of life (70 years) and RF is the risk factor (Sv^{-1}), which reflects the fatal cancer risk per Sievert. For stochastic effects, ICRP 60 uses values of 0.05 for the public (ICRP 1991; Taşkın et al. 2018).

The mean values (± SD) of Ra$_{eq}$, D_R, AEDE and ELCR radiological risk levels calculated for each district in the study area are presented in Fig. 3. The highest average risk levels are shown in the Durağan district, and the lowest average risk levels in the Saraydüzü district. Mean risk values for the Dikmen and Durağan districts were determined to be higher than the provincial average, while the average risk levels of the Gerze and Boyabat districts are close to the provincial average. The mean values of Ra$_{eq}$, D_R, AEDE and ELCR radiological risk levels for the entire working area were calculated to be 62.74 Bq kg^{-1}, 30.51 nGy h^{-1}, 0.04 mSv year^{-1} and 0.13×10^{-3}, respectively. The mean value of Ra$_{eq}$ is lower than the recommended maximum value of 370 Bq kg^{-1}, and the mean values of D_R and AEDE are lower than the world mean value (60 nGy h^{-1} and 0.080 mSv year^{-1}, respectively) (UNSCEAR 2000). The mean values of ELCR in all researched stations are lower than the world's average value (0.29×10^{-3}) (Taskin et al. 2009).

The mean values (± SD) of H_{in}, H_{ex} and $I_{\gamma r}$ radiological index levels for all districts and provinces in the study area are presented comparatively in Fig. 4. Similar to the results shown in Fig. 3, the highest risk indices are found for the Durağan district, and the lowest risk indices for the Saraydüzü district. The radiological index values for Boyabat, Dikmen and Durağan districts were higher than the mean value for all districts. The mean values of the H_{in}, H_{ex} and $I_{\gamma r}$ radiological risk indices for the entire working area were calculated as 0.21, 0.17 and 0.47, respectively. All values of H_{in}, H_{ex} and $I_{\gamma r}$ were calculated to be lower than the criterion value (< 1) (Shohda et al. 2018). Parameters for radiological risk levels are presented in Table 2 as a statistical summary for each district and province.

Interpolated mapping of radionuclide activities

In order to properly map the distributions of the radionuclides, it is necessary to determine the positional correlation between the stations and thus to estimate the activity values of the unmeasured intermediate zones. At this stage, it is important that the data for each station in the study area have normal distribution characteristics (Krige 1966; McGrath et al. 2004); otherwise, the structure of the variogram, which is an indicator of the spatial correlation, may be distorted, leading to a miscalculation of the kriging weights. Histogram curves for the entire working area are presented in Fig. 5. According to these histograms and the results of the Shapiro-Wilk normality test, it was determined that the artificial radionuclide (^{137}Cs) shows a log-normal distribution, while the natural radionuclides (^{226}Ra, ^{232}Th and ^{40}K) show a normal distribution for the entire working area. Therefore, log-transformed values of ^{137}Cs activity results should be used in spatial analysis calculations. At this stage, natural radionuclides do not need transformation, since they have a normal distribution.

Figure 6 shows descriptive diagrams of the cross-validation results and estimation results based on actual measured values for predicted data using the OK approach for natural and artificial radionuclides. For cross-validation, the result of a radiological measurement at a station is excluded from the dataset, and the activity result of this station was estimated using the kriging model generated based on the other measurement results. This process was then applied to all points in the dataset. The descriptive diagrams for each radionuclide are as follows: maps of residuals, showing the magnitudes of prediction errors; cross-validation, showing the relationship between the actual and estimated values: residual vs. predicted data, showing that the errors are independent of the predicted values; and histograms of

residuals, showing the distribution of errors. In the maps of residuals, prediction errors for the entire working area were determined to be generally small. In the cross-validation diagrams, there is a good correlation between the actual measurement results and the predicted values, except for a few outliers. This suggests that the calculated estimation results are appropriate and reliable. In addition, the random and homogeneous distribution of errors in the residuals vs. predicted data diagram shows the normal distribution feature by adding errors close to "0" in the histogram of residual diagram, showing the reliability and appropriateness of the estimates obtained as a result of OK calculations. The results in Fig. 6 show that the OK model proposed for this study area can be used to determine radiological distributions.

Radiographic maps of the activity distribution of ^{226}Ra, ^{232}Th, ^{40}K and ^{137}Cs radionuclides are presented in Fig. 7. In the creation of these maps, the study area was divided into 100×100 m^2 (1-ha spatial resolution) cells and was represented by a grid system. Then, based on the parameters used in the cross-validation process, estimates of the activity levels of natural and artificial radionuclides were calculated for each grid point, and the results were coloured as a distribution map. When the distribution maps were examined, it was determined that the activity concentrations of natural radionuclides (^{226}Ra, ^{232}Th, ^{40}K) were distributed at a high level in the Durağan district (southeast of Sinop), and the activity concentration of the artificial radionuclide (^{137}Cs) was at a high level in the inner and northern areas.

Conclusions

The activity concentrations of the natural (^{226}Ra, ^{232}Th, ^{40}K) and artificial (^{137}Cs) radionuclides were
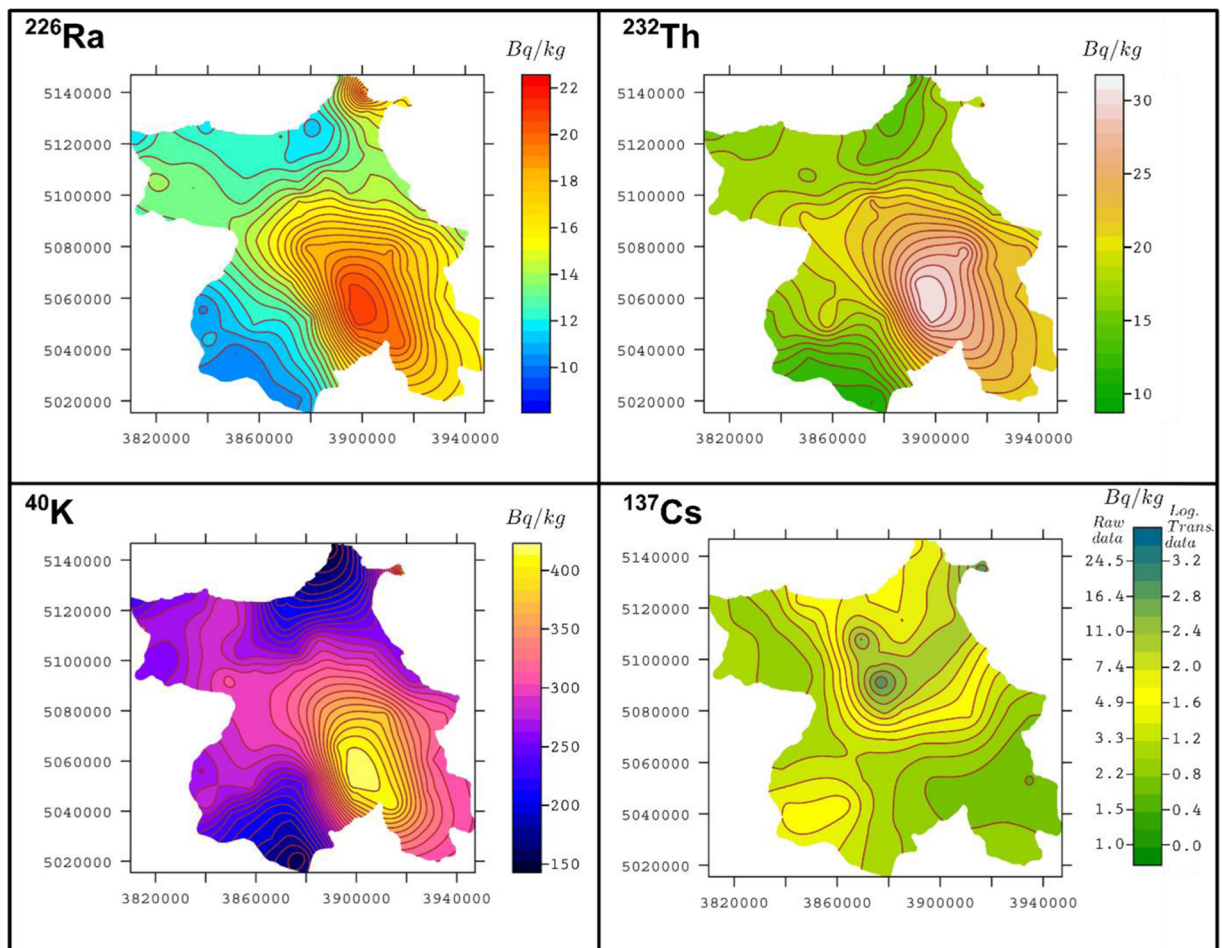

Fig. 7 Interpolated estimation maps for the activity distributions of ^{226}Ra, ^{232}Th, ^{40}K and ^{137}Cs radionuclides

determined by gamma ray spectroscopy in 88 different soil samples collected around the site of the Sinop NPP in Turkey, which is under construction. The mean activity concentrations of ^{226}Ra, ^{232}Th, ^{40}K and ^{137}Cs in the soils were determined to be 14.22, 18.93, 278.62 and 4.37 Bq kg^{-1}, respectively. These values were found to be lower than the world average values. The values of Ra$_{eq}$, D_R, AEDE, ELCR, H_{in}, H_{ex} and $I_{\gamma r}$ were calculated for each site in the study area. These values were determined to be lower than the recommended safety limits.

Using the OK method based on the results of measurements in the study area, predicted values were also calculated for the unmeasured regions, and the performance of the results was evaluated using cross-validation diagrams. The distributions of both natural and artificial radionuclide levels are shown using interpolated estimation maps. According to these maps, it is observed that the activity concentrations of ^{226}Ra, ^{232}Th and ^{40}K are high in the south-eastern parts of the study area, and that of ^{137}Cs is high in the central and northern parts. As a result, it was observed that these soils do not present any significant health risk to humans in this area. These data will be also useful as a baseline for monitoring future changes in radioactivity in the environment of the Sinop NPP.

References

Abba, H. T., Hassan, W. M. S. W., Saleh, M. A., Aliyu, A. S., & Ramli, A. T. (2017). Terrestrial gamma radiation dose (TGRD) levels in northern zone of Jos Plateau, Nigeria: Statistical relationship between dose rates and geological formations. *Radiation Physics and Chemistry, 140*, 167–172. https://doi.org/10.1016/j.radphyschem.2017.01.023.

Baltas, H., Kiris, E., Ustabas, I., Yilmaz, E., Sirin, M., Kuloglu, E., & Gunes, B. E. (2014). Determination of natural radioactivity levels of some concretes and mineral admixtures in Turkey. *Asian Journal of Chemistry, 26*(13), 3946–3952. https://doi.org/10.14233/ajchem.2014.16045.

Baltas, H., Kiris, E., & Sirin, M. (2017). Determination of radioactivity levels and heavy metal concentrations in seawater, sediment and anchovy (Engraulis encrasicolus) from the Black Sea in Rize, Turkey. *Marine Pollution Bulletin, 116*(1–2). doi:https://doi.org/10.1016/j.marpolbul.2017.01.016.

Baltas, H., Sirin, M., Dalgic, G., & Cevik, U. (2018). An overview of the ecological half-life of the 137Cs radioisotope and a

determination of radioactivity levels in sediment samples after Chernobyl in the Eastern Black Sea, Turkey. *Journal of Marine Systems, 177*, 21–27.

Beretka, J., & Mathew, P. J. (1985). Natural radioactivity of Australian building materials, industrial wastes and by-products. *Health physics, 48*(1), 87–95.

Brahmanandhan, G., Selvasekarapandian, S., Malathi, J., Khanna, D., Rajan, M., & Hegde, A. (2007). Natural radioactivity in the soil samples in and around Kudankulam nuclear power plant site. *Journal of Radioanalytical and Nuclear Chemistry, 274*(2), 361–366.

Cafaro, C., Bossew, P., Giovani, C., & Garavaglia, M. (2014). Definition of radon prone areas in Friuli Venezia Giulia region, Italy, using geostatistical tools. *Journal of environmental radioactivity, 138*, 208–219.

Clark, I. (1979). *Practical geostatistics (Vol. 3)*. London: Applied Science Publishers.

Currie, L. A. (1968). Limits for qualitative detection and quantitative determination, Application to radiochemistry. *Analytical chemistry, 40*(3), 586–593.

Diggle, P. J., & Ribeiro, P. J., Jr. (2007). *Model based geostatistics*. New York: Springer.

Durusoy, A., & Yildirim, M. (2017). Determination of radioactivity concentrations in soil samples and dose assessment for Rize Province, Turkey. *Journal of Radiation Research and Applied Sciences, 10*, 348–352.

El Samad, O., Baydoun, R., Nsouli, B., & Darwish, T. (2013). Determination of natural and artificial radioactivity in soil at North Lebanon province. *Journal of Environmental Radioactivity, 125*, 36–39.

Elsaman, R., Omer, M. A. A., Seleem, E. M. M., & El-Taher, A. (2018). Natural radioactivity levels and radiological hazards in soil samples around Abu Karqas Sugar Factory. *Journal of Environmental Science and Technology, 11*(1), 28–38.

Hiemstra, P. H., Pebesma, E. J., Twenhöfel, C. J. W., & Heuvelink, G. B. M. (2009). Real-time automatic interpolation of ambient gamma dose rates from the Dutch radioactivity monitoring network. *Computers & Geosciences, 35*(8), 1711–1721.

Holm, E., & Ballestra, S. (1989). *Measurement of radionuclides in food and the environment, A Guidebook*. Vienna, Ser: IAEA Tech. Rept.

Hung, N. Q., Chuong, H. D., Thanh, T. T., & Van Tao, C. (2016). Intercomparison NaI (Tl) and HPGe spectrometry to studies of natural radioactivity on geological samples. *Journal of environmental radioactivity, 164*, 197–201.

Ihaka, R., & Gentleman, R. (1996). R: A language for data analysis and graphics. *Journal of Computational and Graphical Statistics, 5*(3), 299–314.

İnal, C., & Yiğit, C. Ö. (2003). *Jeodezik uygulamalarda kriging enterpolasyon yönteminin kullanılabilirliği* (pp. 177–185). *Konya*: Coğrafi Bilgi Sistemleri ve Jeodezik Ağlar Çalıştayı.

Kam, E., Bozkurt, A., & Ilgar, R. (2010). A study of background radioactivity level for Canakkale, Turkey. *Environmental Monitoring and Assessment, 168*, 685–690.

Karadeniz, Ö., Karakurt, H., & Akal, C. (2015). Natural radionuclide activities in forest soil horizons of Mount IDA/Kazdagi, Turkey. *Environmental Monitoring and Assessment, 187*, 319.

Kayakökü, H., & Doğru, M. (2017). Radioactivity analysis of soil samples taken from the western and northern shores of Lake Van, Turkey. *Applied Radiation and Isotopes, 128*, 231–236.

Kobya, Y., Taşkın, H., Yeşilkanat, C. M., Çevik, U., Karahan, G., & Çakır, B. (2015). Radioactivity survey and risk assessment study for drinking water in the Artvin province, Turkey. *Water, Air, & Soil Pollution, 226*(3), 49.

Krige, D. G. (1966). Two-dimensional weighted moving average trend surfaces for ore evaluation. South African Institute of Mining and Metallurgy Johannesburg.

Krieger, R. (1981). Radioactivity of construction materials. *Betonwerk Fertigteil Techn, 47*(468).

Kucukomeroglu, B., Karadeniz, A., Damla, N., Yesilkanat, C. M., & Cevik, U. (2016). Radiological maps in beach sands along some coastal regions of Turkey. *Marine pollution bulletin, 112*(1), 255–264.

Kurnaz, A., Kucukomeroglu, B., Damla, N., & Cevik, U. (2011). Radiological maps for Trabzon, Turkey. *Journal of Environmental Radioactivity, 102*, 393–399.

Leelőssy, Á., Mészáros, R., & Lagzi, I. (2011). Short and long term dispersion patterns of radionuclides in the atmosphere around the Fukushima Nuclear Power Plant. *Journal of environmental radioactivity, 102*(12), 1117–1121.

Li, C., Lu, Z., Ma, T., & Zhu, X. (2009). A simple kriging method incorporating multiscale measurements in geochemical survey. *Journal of Geochemical Exploration, 101*(2), 147–154.

Lukšienė, B., Marčiulionienė, D., Rožkov, A., Gudelis, A., Holm, E., & Galvonaitė, A. (2012). Distribution of artificial gamma-ray emitting radionuclide activity concentration in the top soil in the vicinity of the Ignalina Nuclear Power Plant and other regions in Lithuania. *Science of the total environment, 439*, 96–105.

Matheron, G. (1970). Random structures and mathematical geology. *REVUE DE L INSTITUT INTERNATIONAL DE STATISTIQUE-REVIEW OF THE INTERNATIONAL STATISTICAL INSTITUTE, 38*(1), 1.

McGrath, D., Zhang, C., & Carton, O. T. (2004). Geostatistical analyses and hazard assessment on soil lead in Silvermines area, Ireland. *Environmental Pollution, 127*(2), 239–248.

Mičieta, K., & Murín, G. (2007). Wild plant species in bio-indication of radioactive-contaminated sites around Jaslovske Bohunice nuclear power plant in the Slovak Republic. *Journal of Environmental radioactivity, 93*(1), 26–37.

Olea, R. A. (1982). *Optimization of the high plains aquifer observation network*. Kansas: Kansas Geological Survey.

Oliver, M. A., & Webster, R. (2014). A tutorial guide to geostatistics: Computing and modelling variograms and kriging. *Catena, 113*, 56–69.

Pebesma, E. J., & Bivand, R. S. (2005). Classes and methods for spatial data in R. *R news, 5*(2), 9–13.

Pebesma, E. J., & Wesseling, C. G. (1998). Gstat: A program for geostatistical modelling, prediction and simulation. *Computers & Geosciences, 24*(1), 17–31.

Protection, I. C. on R. (1991). ICRP Publication 60: 1990 Recommendations of the international commission on radiological protection. Elsevier Health Sciences.

Radiation, U. N. S. C. on the E. of A. (2000). Sources and effects of ionizing radiation: Sources (Vol. 1). United Nations Publications.

Sanusi, M. S. M., Ramli, A. T., Gabdo, H. T., Garba, N. N., Heryanshah, A., Wagiran, H., & Said, M. N. (2014). Isodose mapping of terrestrial gamma radiation dose rate of Selangor state, Kuala Lumpur and Putrajaya, Malaysia. *Journal of environmental radioactivity, 135*, 67–74.

Savelieva, E. (2005). Using ordinary kriging to model radioactive contamination data. *Applied GIS, 1*(2), 1–10.

Shohda, A. M., Draz, W. M., Ali, F. A., & Yassien, M. A. (2018). Natural radioactivity levels and evaluation of radiological hazards in some Egyptian ornamental stones. *Journal of Radiation Research and Applied Sciences, 11*, 323–327.

Taskin, H., Karavus, M., Ay, P., Topuzoglu, A., Hidiroglu, S., & Karahan, G. (2009). Radionuclide concentrations in soil and lifetime cancer risk due to gamma radioactivity in Kirklareli, Turkey. *Journal of environmental radioactivity, 100*(1), 49–53.

Taşkın, H., Yeşilkanat, C. M., Kobya, Y., & Çevik, U. (2018). Evaluation and mapping of radionuclides in the terrestrial environment and health hazard due to soil radioactivity in Artvin, Turkey. *Arabian Journal of Geosciences, 11*(23), 729. https://doi.org/10.1007/s12517-018-4063-8.

Team, R. D. C. (2005). *R: A language and environment for statistical computing, reference index version 2.9. 2*. Vienna, Austria: R Foundation for Statistical Computing ISBN 3–900051-07-0, URL http://www. rproject. org.

Tsai, T.-L., Lin, C.-C., Wang, T.-W., & Chu, T.-C. (2008). Radioactivity concentrations and dose assessment for soil samples around nuclear power plant IV in Taiwan. *Journal of radiological protection, 28*(3), 347.

Warnery, E., Ielsch, G., Lajaunie, C., Cale, E., Wackernagel, H., Debayle, C., & Guillevic, J. (2015). Indoor terrestrial gamma dose rate mapping in France: a case study using two different geostatistical models. *Journal of environmental radioactivity, 139*, 140–148.

Webster, R., & Oliver, M. A. (2001). Geostatistics for environmental scientists (Statistics in Practice).

Yeşilkanat, C. M., Kobya, Y., Taşkın, H., & Çevik, U. (2015). Dose rate estimates and spatial interpolation maps of outdoor gamma dose rate with geostatistical methods: A case study from Artvin, Turkey. *Journal of environmental radioactivity, 150*, 132–144.